NACA RM L51B16

NACA

RESEARCH MEMORANDUM

WIND-TUNNEL INVESTIGATION AT SUBSONIC AND LOW TRANSONIC SPEEDS OF THE EFFECTS OF AILERON SPAN AND SPANWISE LOCATION ON THE ROLLING CHARACTERISTICS OF A TEST VEHICLE WITH THREE UNTAPERED 45° SWEPTBACK WINGS

By Harold S. Johnson

Langley Aeronautical Laboratory
Langley Field, Va.

NATIONAL ADVISORY COMMITTEE
FOR AERONAUTICS

WASHINGTON

April 6, 1951

NATIONAL ADVISORY COMMITTEE FOR AERONAUTICS

RESEARCH MEMORANDUM

WIND-TUNNEL INVESTIGATION AT SUBSONIC AND LOW TRANSONIC SPEEDS OF THE EFFECTS OF AILERON SPAN AND SPANWISE LOCATION ON THE ROLLING CHARACTERISTICS OF A TEST VEHICLE WITH THREE UNTAPERED 45° SWEPTBACK WINGS

By Harold S. Johnson

SUMMARY

A wind-tunnel investigation was made through a Mach number range of 0.30 to about 0.94 to determine the rolling characteristics of a three-winged free-flight type of test vehicle having untapered 45° sweptback wings of NACA 65A009 airfoil sections and equipped with 0.20-chord ailerons having various spans and spanwise locations. The aspect ratio based on the area of two wings was 3.7.

The wing-tip helix angles, rolling-moment coefficients, and damping-in-roll coefficients were generally only slightly affected by Mach number variations for the range covered in the investigation. A partial-span aileron was most effective when at a midsemispan location and least effective when located at the wing tip. The aileron effectiveness parameters and the damping-in-roll coefficients were in good agreement with theory. The results are in good agreement with data obtained by the free-flight rocket-propelled and transonic-bump testing techniques.

INTRODUCTION

The need for lateral-control design data in the transonic speed range has led to the establishment by the National Advisory Committee for Aeronautics of an integrated program for transonic research. The experimental data for this program are being obtained through the use of different testing methods, each of which has its limitations with regard to such factors as Mach number range, Reynolds number, and type and size of model. One testing technique consists of firing free-flight

rocket-propelled test vehicles having preset deflected ailerons. From transmitted records of the flight, the variations of wing-tip helix angle and drag coefficient with Mach number are obtained.

This paper presents the results of a wind-tunnel investigation of such a test vehicle made to determine the effects of aileron span and spanwise aileron location on the rolling characteristics and, in addition, to compare the rolling effectiveness of three of the aileron configurations with corresponding data obtained by the free-flight testing method. The three-winged test vehicle was mounted on a free-roll sting support in the Langley 300-MPH and high-speed 7- by 10-foot tunnels. The investigation covered a Mach number range of from 0.3 to about 0.94.

COEFFICIENTS AND SYMBOLS

$pb/2V$	wing-tip helix angle, radians
C_l	rolling-moment coefficient (L/qSb)
C_{l_p}	damping-in-roll coefficient $\left(-\frac{C_l}{pb/2V}\right)$
L	rolling moment resulting from aileron deflection, foot-pounds
p	rolling velocity resulting from aileron deflection, radians per second
b	diameter of circle swept by wing tips (with regard to rolling characteristics, this diameter is considered to be the effective wing span of the test vehicle), 2.184 feet
S	total wing area (wings assumed to extend to model center line), 1.931 square feet
V	free-stream or flight-path velocity, feet per second
q	dynamic pressure, pounds per square foot $\left(\frac{\rho V^2}{2}\right)$
ρ	mass density of air, slugs per cubic foot
M	Mach number (V/a)
a	speed of sound, feet per second
δ_a	average aileron deflection of three wings relative to wing-chord plane, measured perpendicular to aileron hinge axis, degrees

δ_T twice average aileron deflection (equivalent to the total deflection of the opposite deflected ailerons on a conventional wing configuration), degrees

y_i spanwise distance from model center line to inboard end of aileron, feet

y_o spanwise distance from model center line to outboard end of aileron, feet

b_a aileron span measured perpendicular to model center line, feet

$C_{l_\delta} = \frac{\partial C_l}{\partial \delta_a}$

MODEL AND TESTING TECHNIQUE

The dimensional characteristics of the test vehicle used in the investigation are shown in figure 1. The model consisted of a pointed cylindrical wooden body at the rear of which were attached three aluminum-alloy wings of NACA 65A009 airfoil section (measured parallel to model center line). The three-wing arrangement is used to provide free-flight stability for this type of test vehicle. The wings were untapered and swept back 45°. The aspect ratio (based on the area of two wings measured to model center line) was 3.7.

The interchangeable 20-percent-chord ailerons, having deflections of approximately 0°, 2°, 5°, 10° and 20°, were constructed with joints at three spanwise locations so that various spans of ailerons at various spanwise locations could be investigated (fig. 2). There was no gap between aileron segments when two or more segments were tested in combination. The ailerons were sealed with no surface discontinuity at the hinge axis. The ailerons were deflected simultaneously on all three wings.

The rocket motor was replaced by a steel sting (fig. 1) which extended behind the test vehicle into a free-roll sting support located downstream from the test section. For the high-speed-tunnel tests, the sting support was attached to a vertical strut which was part of the tunnel balance system. Both the strut and a part of the sting support were shielded from the air stream by a fairing. A photograph of the installation is shown in figure 3. The high-speed-tunnel rolling-moment data were obtained from tunnel balance measurements with the sting restrained in roll. For the tests in the Langley 300 MPH 7- by 10-foot tunnel, the sting support was mounted on a vertical strut which was

attached to the tunnel floor and ceiling. The rolling moments were measured by a calibrated electrical-resistance strain gage with the sting restrained in roll by the strain gage. In both tunnels the rolling velocities were electrically recorded. A more complete description of the high-speed-tunnel free-roll testing equipment is given in references 1 and 2. From the measured data, rolling-moment coefficients, wing-tip helix angles, and damping-in-roll coefficients were obtained for a Mach number range of from 0.30 to about 0.94.

The angle of attack was 0° for all tests. The aileron deflection range investigated was from 0° to about 20° at a Mach number of 0.30 but was limited to 5° or 10° for Mach numbers greater than 0.30. In addition to the full-span aileron $\left(b_a = 0.809\frac{b}{2}\right)$, three partial-span outboard ailerons $\left(y_o = 1.000\frac{b}{2}\right)$, three partial-span inboard ailerons $\left(y_i = 0.191\frac{b}{2}\right)$, and the $0.405\frac{b}{2}$ aileron at the midsemispan location $\left(y_o = 0.798\frac{b}{2},\ y_i = 0.393\frac{b}{2}\right)$ were tested. (See table I and fig. 2.) The variation of Reynolds number with Mach number for average test conditions is shown in figure 4.

CORRECTIONS

The rolling-moment coefficients, wing-tip helix angles, and Mach numbers have been corrected for blockage by the model and its wake by the method of reference 3. The coefficients have not been corrected for the effects of tares. Tests of other sting-supported models in the high-speed tunnel have shown the tare corrections to rolling-moment coefficients to be negligible. The rolling velocities have been corrected for the small bearing-friction losses. No corrections have been applied to the data to account for the effects of wing distortion under load; however, a discussion of these distortion effects is included in following sections of this paper. The change in aileron deflection resulting from load was negligible. The model had a small amount of wing incidence and twist and initial aileron deflection resulting from constructional limitations. The data were corrected to a wing incidence of 0° and no twist by subtracting the data obtained with the ailerons at the initial deflection from the data obtained with the ailerons deflected. The aileron deflection given is the incremental difference between the deflected aileron and the aileron at the initial deflection.

RESULTS AND DISCUSSION

Presentation of Data

The effects of aileron span and spanwise location on the variation of the rolling characteristics $pb/2V$, C_l, and C_{l_p} with aileron deflection and Mach number are presented in figures 5 to 9. Also shown in figures 6(a) and 6(b) is a comparison of theoretical and experimental values of C_{l_p}. A comparison of the experimental values of $\frac{pb/2V}{\delta_T}$ with those obtained from free-flight rocket-propelled tests of similar models is shown in figure 10. The effects of aileron span and spanwise location on the aileron effectiveness parameter C_{l_δ} are presented in figures 11 and 12. A comparison of the experimental and estimated C_{l_δ} values is shown in figure 13. The experimental C_{l_δ} values are compared in figure 14 with those obtained for a similar model by using the transonic-bump testing technique.

Wing-Tip Helix Angles

For all spans of ailerons at the various spanwise locations investigated, the variation of $pb/2V$ with aileron deflection was very nearly linear for values of δ_a of less than about 10° (figs. 5 to 8). The $pb/2V$ values generally decreased slightly with increasing Mach numbers and this decrease became more pronounced at the higher Mach numbers ($M > 0.85$). These Mach number effects were less pronounced when the aileron was at the inboard $\left(y_i = 0.191\frac{b}{2}\right)$ location. The variation of $pb/2V$ with aileron span was generally nonlinear (figs. 5 to 9). Throughout the Mach number range investigated, the outboard $0.202\frac{b}{2}$ aileron was less effective in proportion to span in producing $pb/2V$ than the larger span outboard ailerons. At low Mach numbers, the inboard $0.202\frac{b}{2}$ aileron was also less effective in proportion to span than the larger-span inboard ailerons. This variation of $pb/2V$ with b_a became less pronounced as the Mach number was increased and was very nearly linear at the highest Mach numbers investigated (fig. 9). A study of figures 7 to 9 indicates that partial-span ailerons located inboard on the wing semispan were more effective than ailerons located at the wing tip and this effect of spanwise location generally became more pronounced as the Mach number was increased. The data for the $0.405\frac{b}{2}$ ailerons show the midsemispan location to be the most effective (figs. 7 and 8(a)).

A comparison of the rolling effectiveness of the test vehicle equipped with inboard and outboard $0.405\frac{b}{5}$ and full-span ailerons with that obtained from free-flight rocket-propelled tests of similar models (reference 4) is shown in figure 10. The rolling effectiveness is expressed as $\frac{pb/2V}{\delta_T}$ because the aileron deflections were not identical and the parameter represents the helix angle resulting from a 1° total-aileron deflection (the summation of the opposite deflected ailerons) on a conventional two-wing configuration. The change in interference effects resulting from the three-wing arrangement has been neglected. (See reference 4.) The comparison shows that the results obtained by the two testing techniques are in good agreement. The wings of the test vehicle used in the wind-tunnel investigation were approximately twice as rigid in torsion as those of the free-flight vehicles. Computations by the method of reference 5 show that wing distortion accounts for most of the difference between the tunnel and free-flight data for the outboard $0.405\frac{b}{2}$ and full-span ailerons. At $M = 0.9$, the computations for the full-span ailerons indicate that the test results are about 6 and 15 percent less than those for a rigid wing for the tunnel and free-flight models, respectively, and the corrected results agree within 0.0002. For the inboard ailerons, the correction for wing distortion would increase the discrepancy but, because the aileron-moment arm is short, the corrections are very small and the maximum difference between the corrected values is about 0.0003.

Rolling-Moment Coefficient

The data of figures 5 to 8 show that the effects of aileron deflection, aileron span, and aileron spanwise location on the rolling-moment coefficients are generally similar to those on the wing-tip helix angles. The rolling-moment coefficients were less affected by Mach number variations than the $pb/2V$ values for the range covered in the investigation.

The aileron-effectiveness parameter C_{l_δ} was relatively unaffected by Mach number variations for the range investigated (figs. 11 and 12). Partial-span ailerons were more effective when located inboard on the wing semispan than at the outboard location (figs. 12, 13, and 14) and the $0.405\frac{b}{2}$ aileron was most effective when at the midsemispan location. The agreement between the experimental and estimated (reference 6) values of C_{l_δ} for the various ailerons investigated is good, although the estimated values are slightly lower than the experimental values for the ailerons having inboard locations and are generally slightly

higher for the outboard ailerons (fig. 13). The data of figure 14 show that the sting-model results generally agree with the results of an investigation of a similar model utilizing the transonic-bump testing method (reference 7). The bump-model data of reference 7 show a more marked reduction of C_{l_δ} with increasing Mach number than was shown by the sting-mounted-model data.

Calculations and loading tests of similar wings have indicated that the loss in rolling-moment coefficient due to distortion under load is about 8 percent at the highest Mach numbers for the model with the full-span aileron deflected 5°. The reduction in rolling moment is greater than the reduction in $pb/2V$ since the root bending moment is not zero as is the case when there is no restraint in roll.

Damping-in-Roll Coefficients

For all the aileron configurations investigated, the damping-in-roll coefficients generally increased slightly with increasing Mach number and this increase became more pronounced at the higher Mach numbers (figs. 6 and 8). Although the variations of C_{l_p} with aileron deflection, span, and spanwise location were generally within the experimental accuracy, C_{l_p} generally decreased as the aileron deflection and span were increased and also when a partial-span aileron was moved inboard from the wing tip (figs. 5 to 8).

The comparison with the theoretical curve of C_{l_p} against Mach number, as determined by the method of reference 8, shows that the magnitude of the experimentally determined C_{l_p} values and their variation with Mach number are in good agreement with those predicted by theory (figs. 6(a) and 6(b)). Since wing distortion under load causes a larger decrease in C_l than in $pb/2V$, the experimental C_{l_p} values are lower than rigid-wing results. The decrease due to distortion is estimated to be about 3 percent for the test vehicle with the full-span ailerons deflected 5° at a Mach number of 0.9.

CONCLUSIONS

A wind-tunnel investigation to determine the effects of aileron span and spanwise location on the rolling characteristics of a three-winged test vehicle having untapered 45° sweptback wings through a Mach number range of 0.30 to about 0.94 indicated the following conclusions:

1. The wing-tip helix angles, rolling-moment coefficients, and damping-in-roll coefficients were generally only slightly affected by Mach number variations for the range covered in the investigation.

2. A partial-span aileron was most effective when at a midsemispan location and least effective when located at the wing tip.

3. The experimentally determined aileron effectiveness parameters and the damping-in-roll coefficients were in good agreement with theoretically determined values.

4. The results are in good agreement with data obtained by the free-flight rocket-propelled and transonic-bump testing techniques.

Langley Aeronautical Laboratory
National Advisory Committee for Aeronautics
Langley Field, Va.

REFERENCES

1. Myers, Boyd C., II, and Kuhn, Richard E.: High-Subsonic Damping-in-Roll Characteristics of a Wing with the Quarter-Chord Line Swept Back 35° and with Aspect Ratio 3 and Taper Ratio 0.6. NACA RM L9C23, 1949.

2. Johnson, Harold S.: Wind-Tunnel Investigation at Low Transonic Speeds of the Effects of Number of Wings on the Lateral-Control Effectiveness of an RM-5 Test Vehicle. NACA RM L9H16, 1949.

3. Herriot, John G.: Blockage Corrections for Three-Dimensional-Flow Closed-Throat Wind Tunnels, with Consideration of the Effects of Compressibility. NACA Rep. 995, 1950.

4. Strass, H. Kurt: The Effect of Spanwise Aileron Location on the Rolling Effectiveness of Wings with 0° and 45° Sweep at Subsonic, Transonic, and Supersonic Speeds. NACA RM L50A27, 1950.

5. Strass, H. Kurt, Fields, E. M., and Purser, Paul E.: Experimental Determination of Effect of Structural Rigidity on Rolling Effectiveness of Some Straight and Swept Wings at Mach Numbers from 0.7 to 1.7. NACA RM L50G14b, 1950.

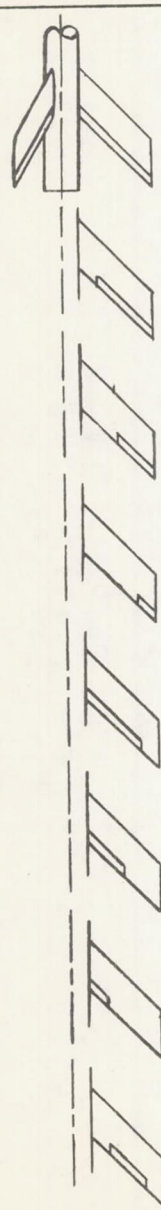
6. Lowry, John G., and Schneiter, Leslie E.: Estimation of Effectiveness of Flap-Type Controls on Sweptback Wings. NACA TN 1674, 1948.

7. MacLeod, Richard G.: Investigation of Flap-Type Ailerons on an Untapered Wing Having an Aspect Ratio of 3.7, 45° Sweepback, and an NACA 65A009 Airfoil Section. Transonic-Bump Method. NACA RM L50G03, 1950.

8. Bird, John D.: Some Theoretical Low-Speed Span Loading Characteristics of Swept Wings in Roll and Sideslip. NACA Rep. 969, 1950.

TABLE I

DIMENSIONAL CHARACTERISTICS OF THE VARIOUS 0.20-CHORD AILERONS

Configuration	Aileron span, $\frac{b_a}{b/2}$	Aileron spanwise location	
		$\frac{y_i}{b/2}$	$\frac{y_o}{b/2}$
	0.809 (full span)	0.191	1.000
	.607	.393	1.000
	.405	.595	1.000
	.202	.798	1.000
	.607	.191	.798
	.405	.191	.595
	.202	.191	.393
	.405	.393	.798

NACA

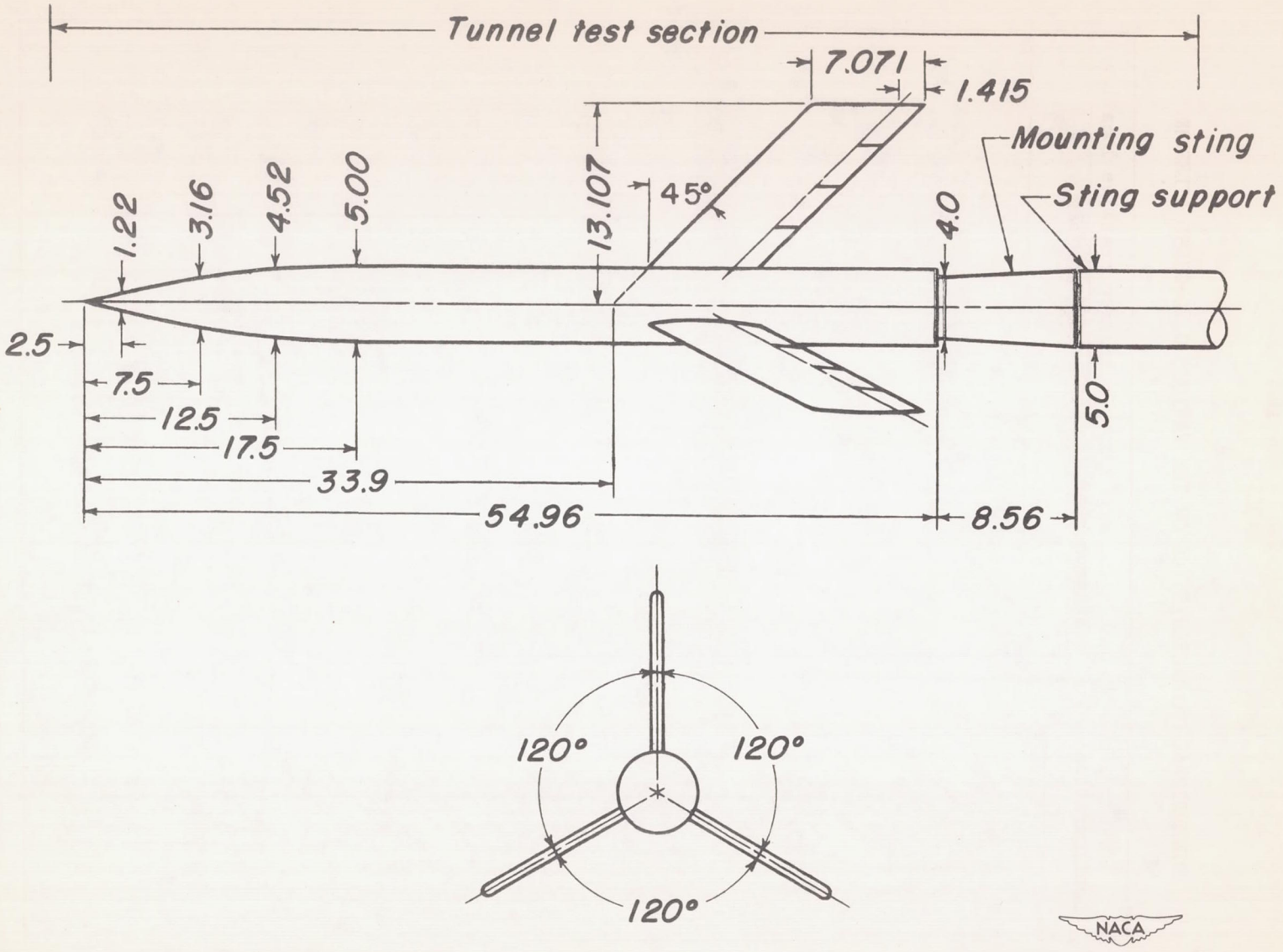


Figure 1.- The test vehicle used for the investigation. (All dimensions are in inches.)

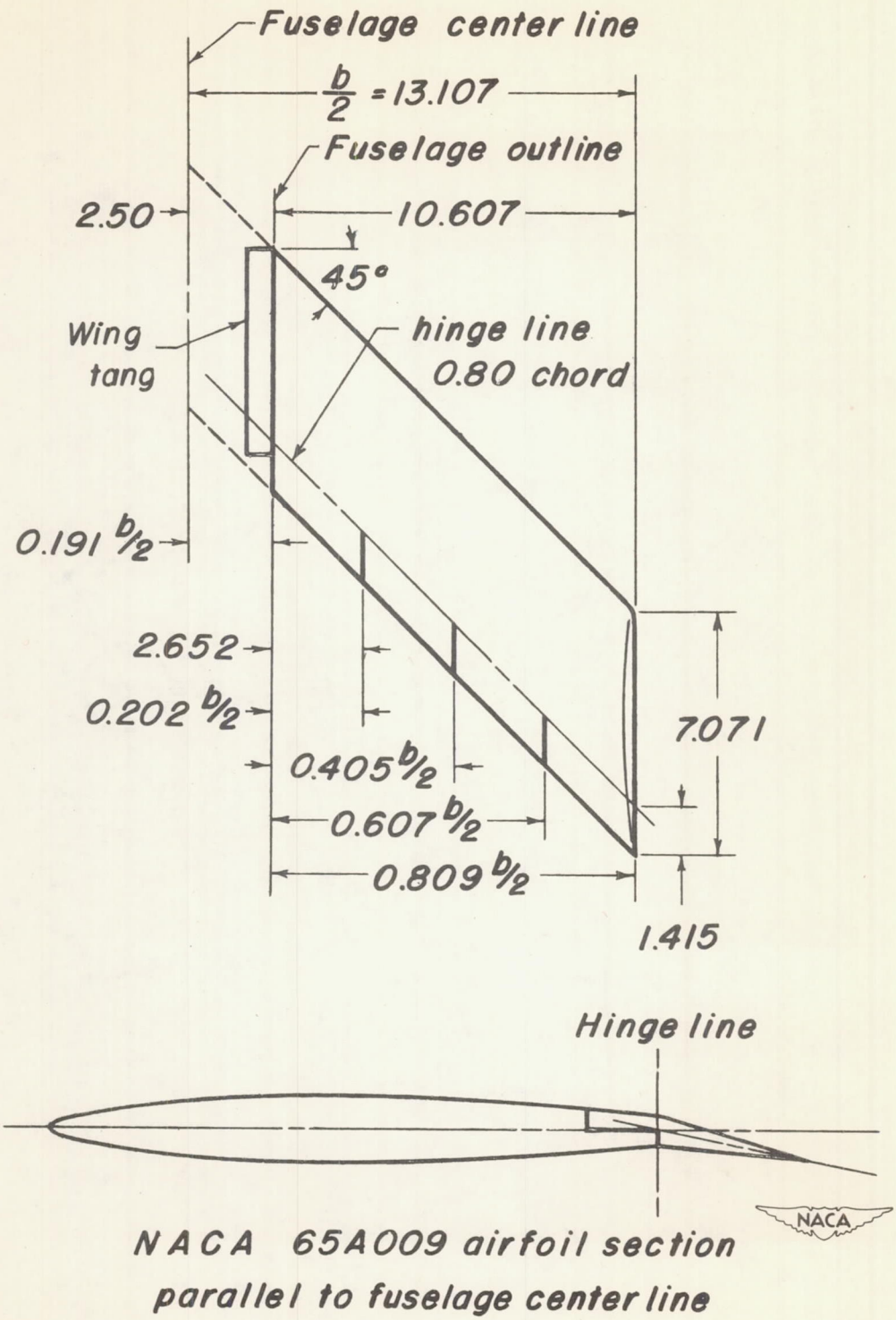


Figure 2.- Details of the wing and ailerons. (All dimensions are in inches.)

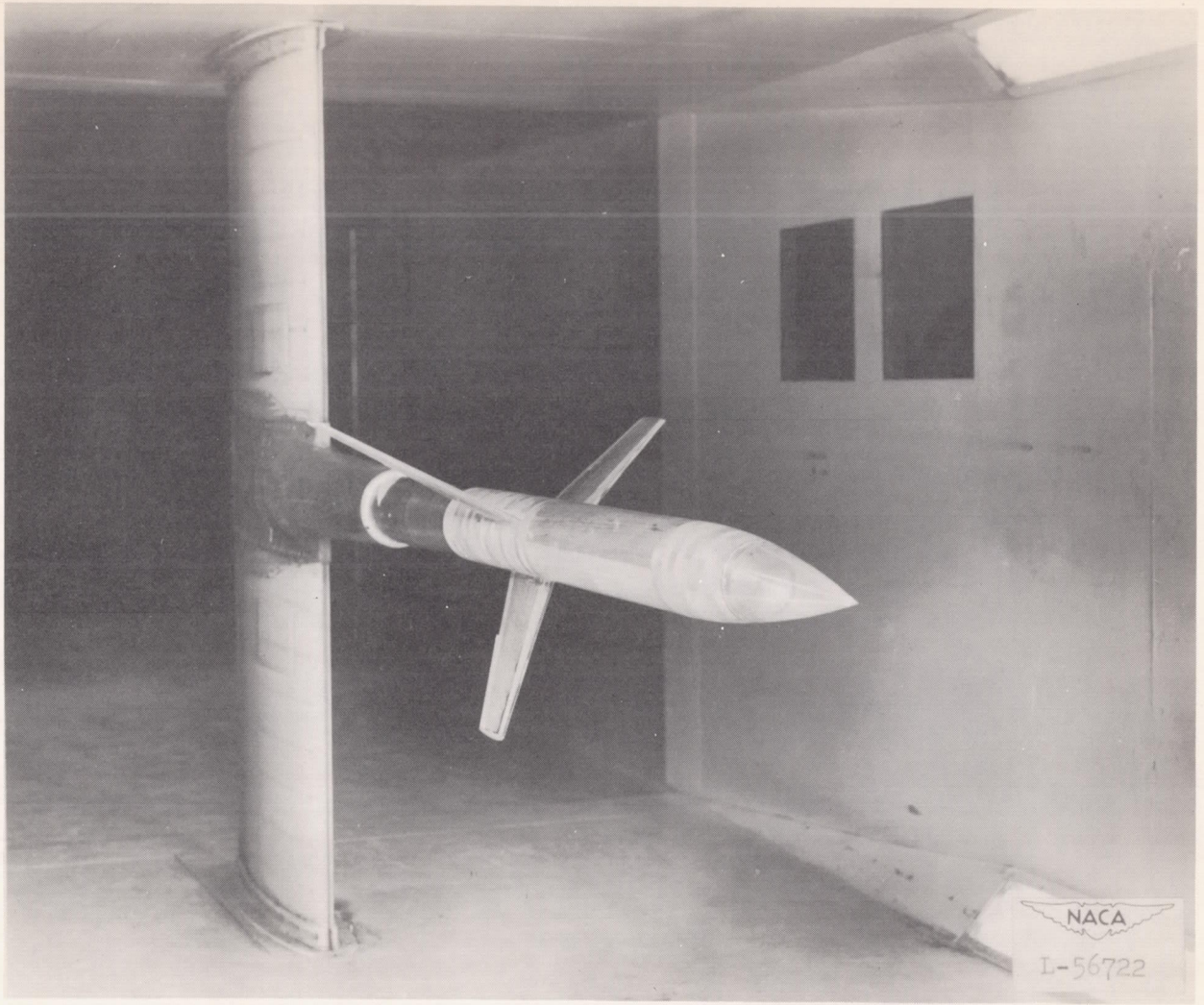


Figure 3.- Photograph of a typical installation in the Langley high-speed 7- by 10-foot tunnel.

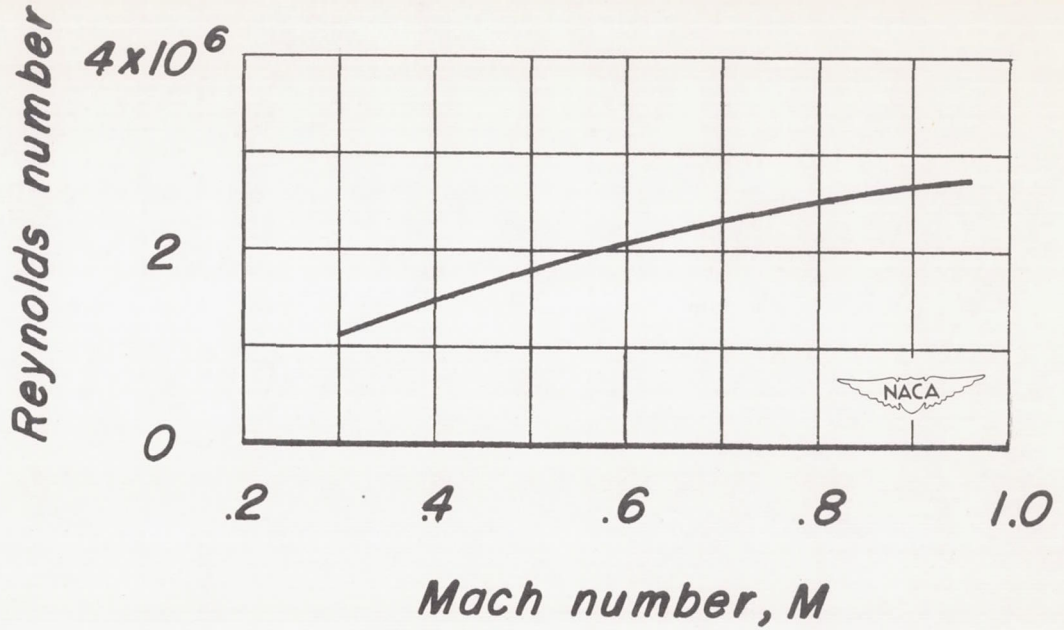


Figure 4.- Variation of average Reynolds number with Mach number.

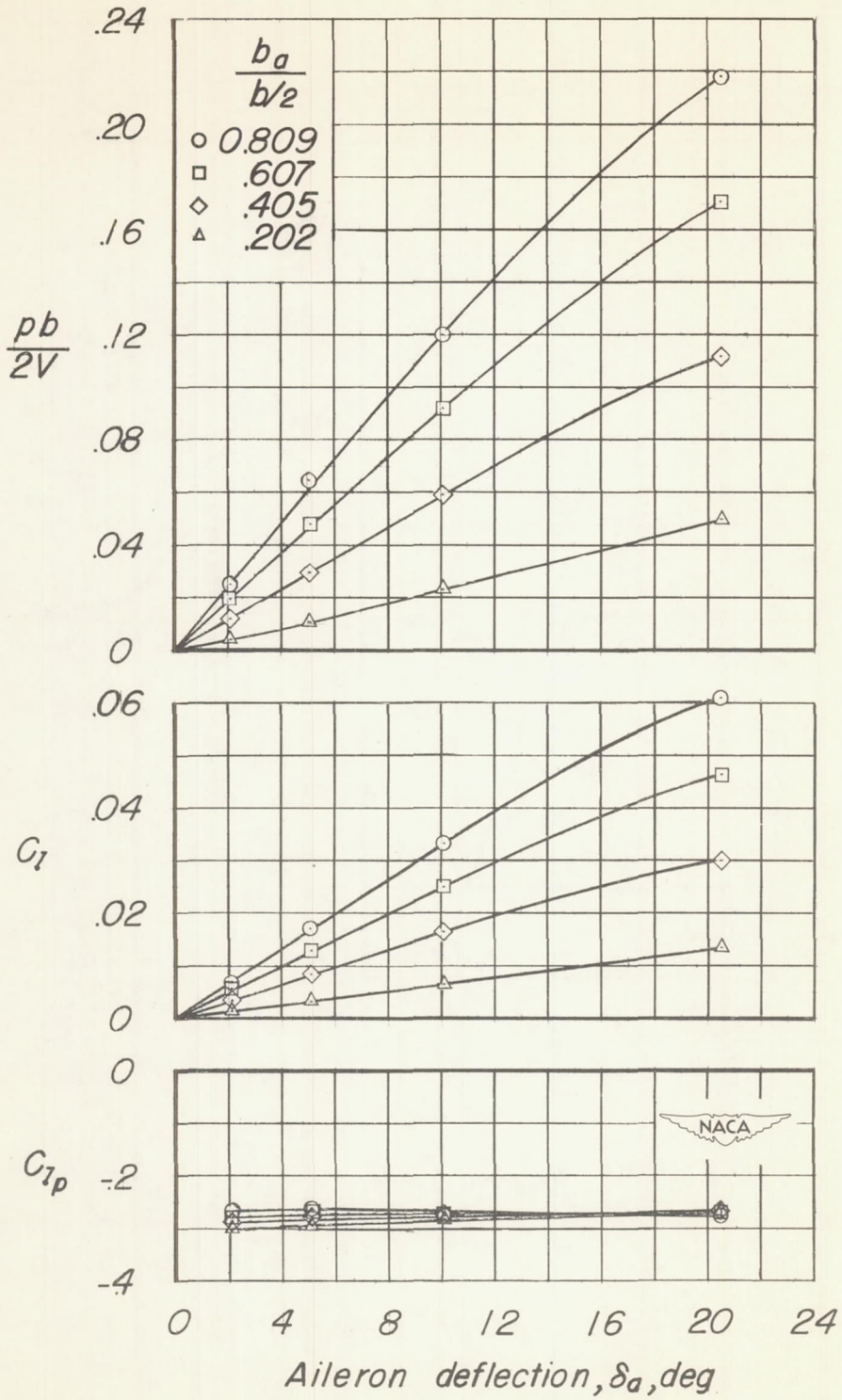
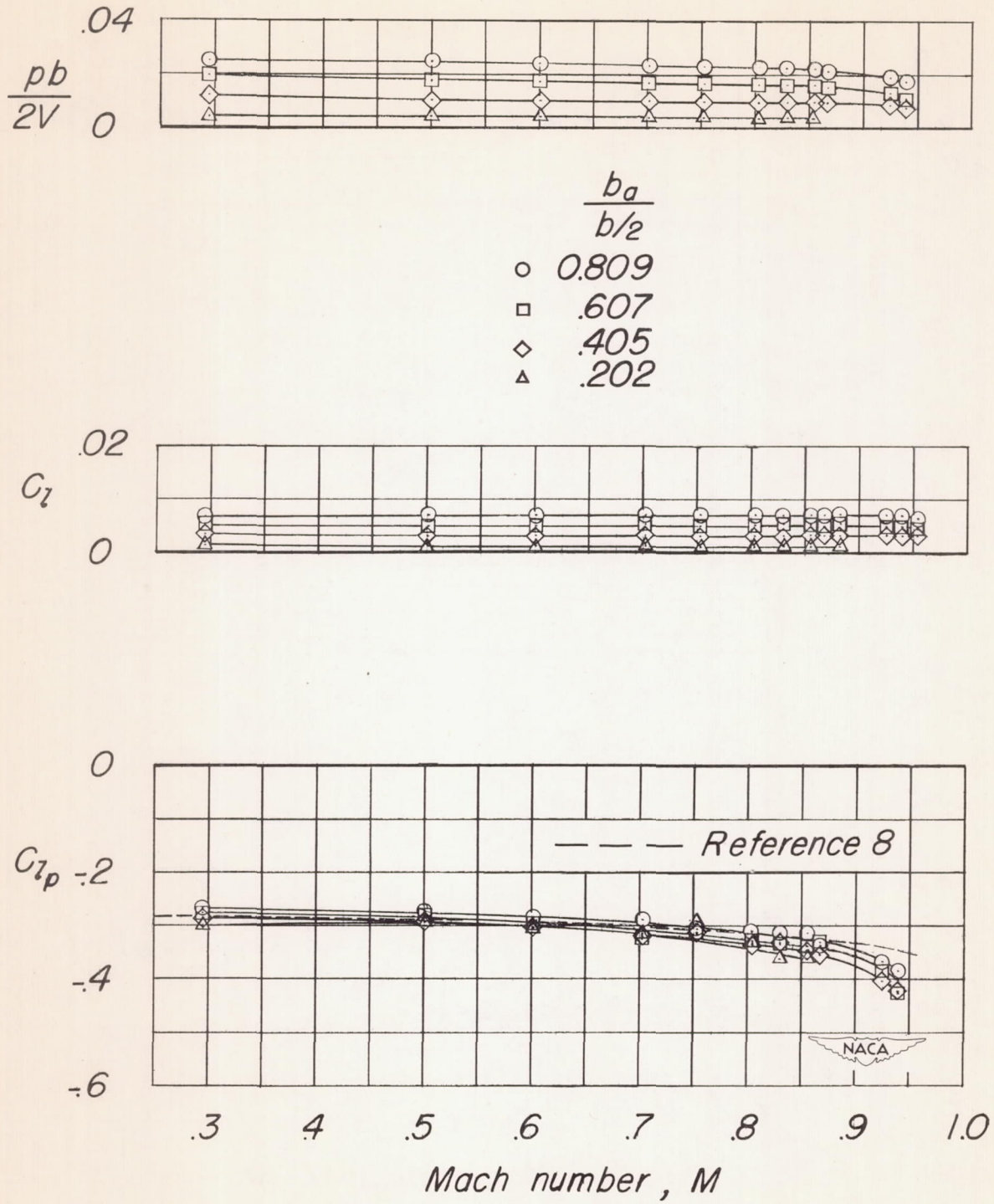
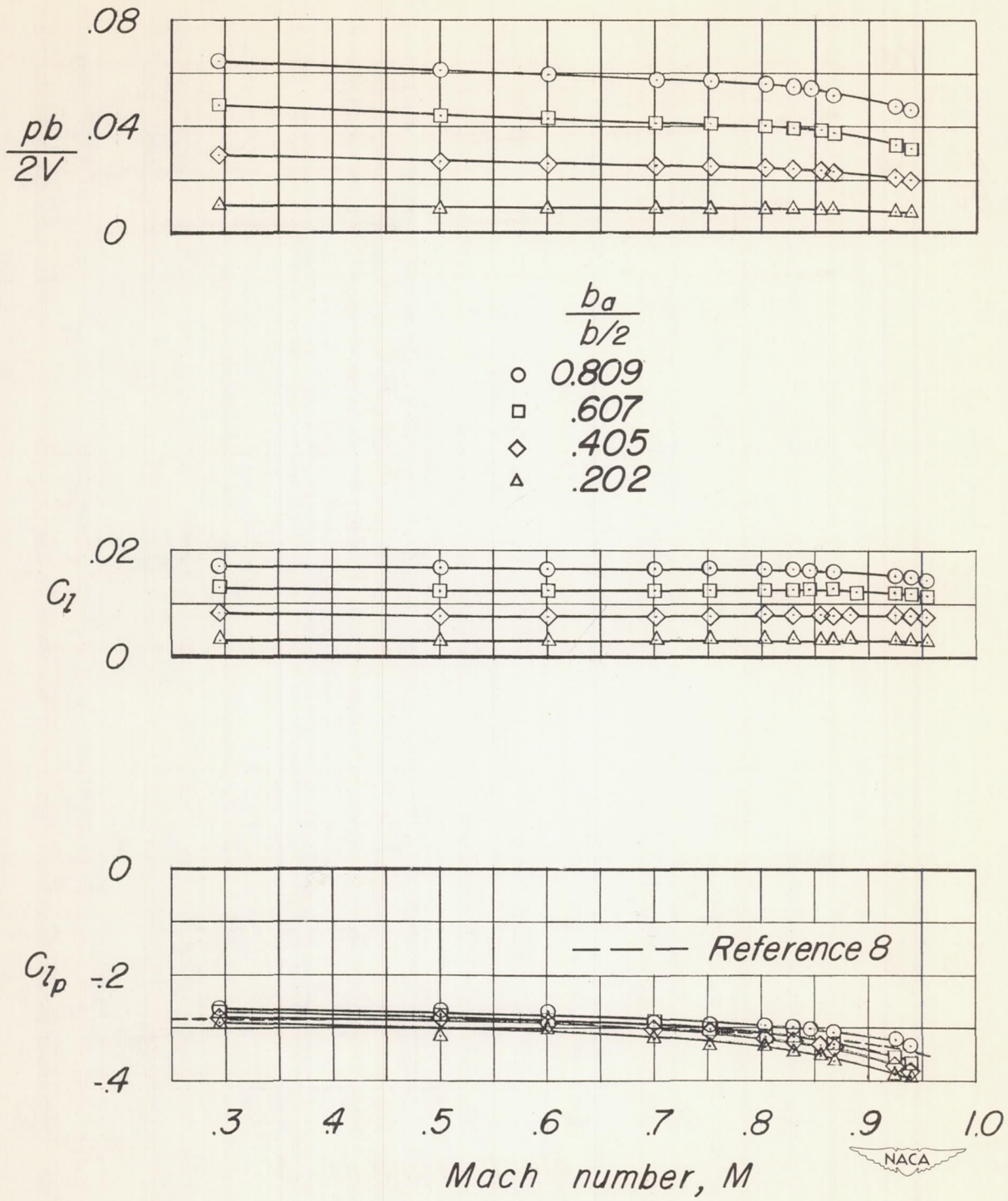


Figure 5.- Effect of aileron span on the variation of the rolling characteristics with aileron deflection. $y_o = 1.000\frac{b}{2}$; M = 0.30.



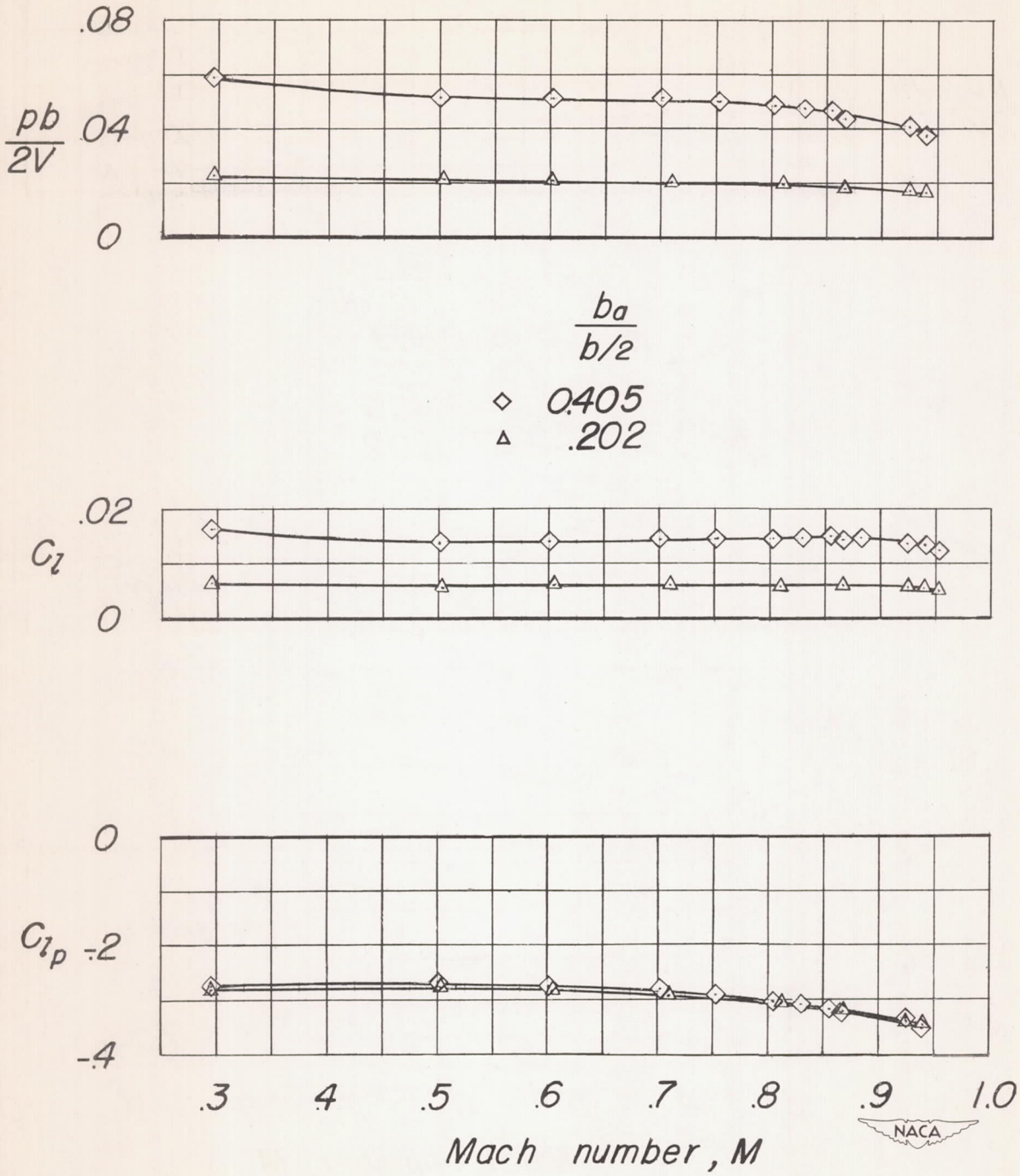
(a) $\delta_a = 2.14^\circ$.

Figure 6.- Effect of aileron span on the variation of the rolling characteristics with Mach number. $y_o = 1.000\frac{b}{2}$.



(b) $\delta_a = 5.07^\circ$.

Figure 6.- Continued.



(c) $\delta_a = 10.06^\circ$.

Figure 6.- Concluded.

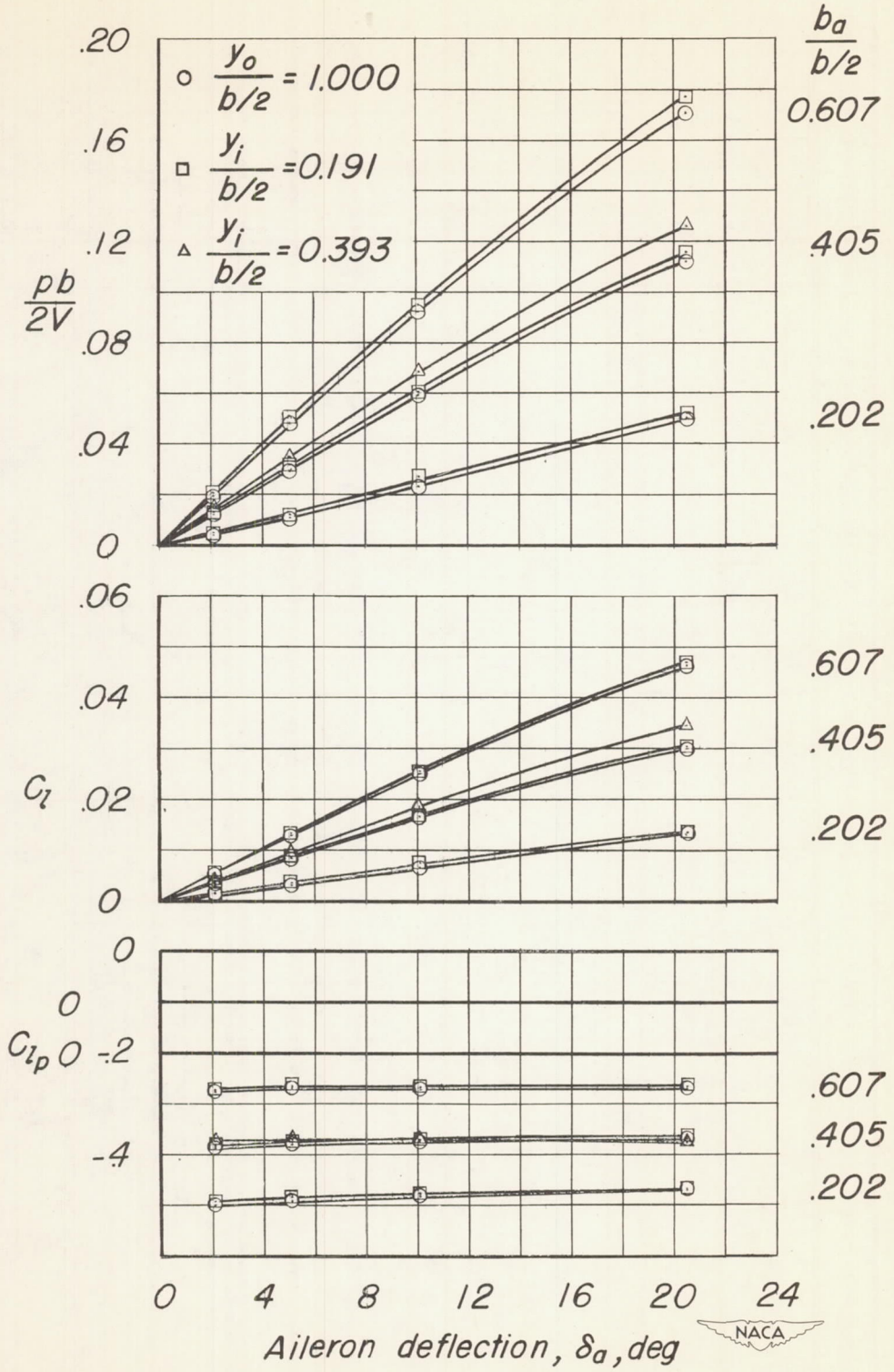
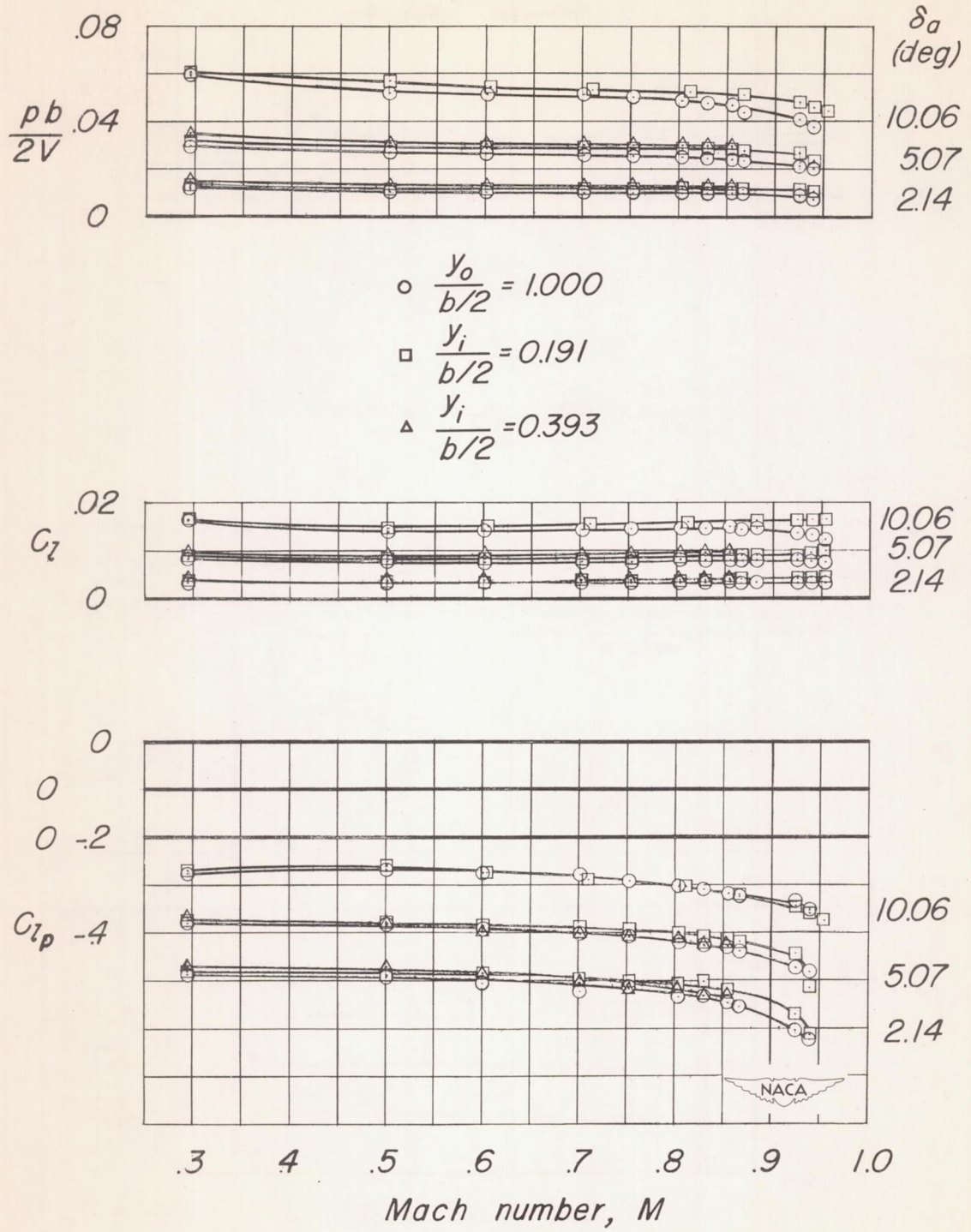
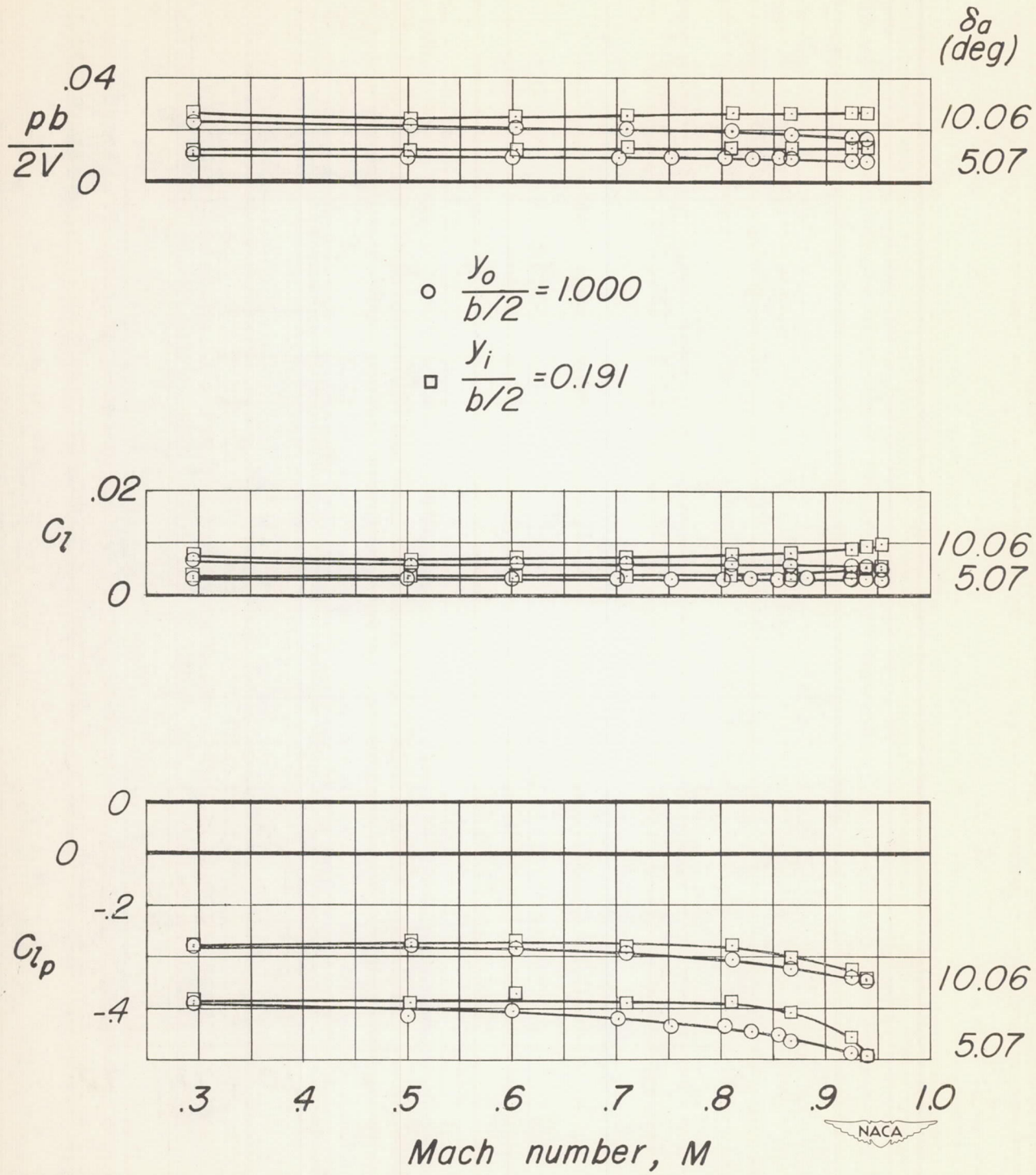


Figure 7.- Effect of spanwise aileron location on the variation of the rolling characteristics with aileron deflection. M = 0.30.



(a) $b_a = 0.405\frac{b}{2}$.

Figure 8.- Effect of spanwise aileron location on the variation of the rolling characteristics with Mach number.



(b) $b_a = 0.202\frac{b}{2}$.

Figure 8.- Concluded.

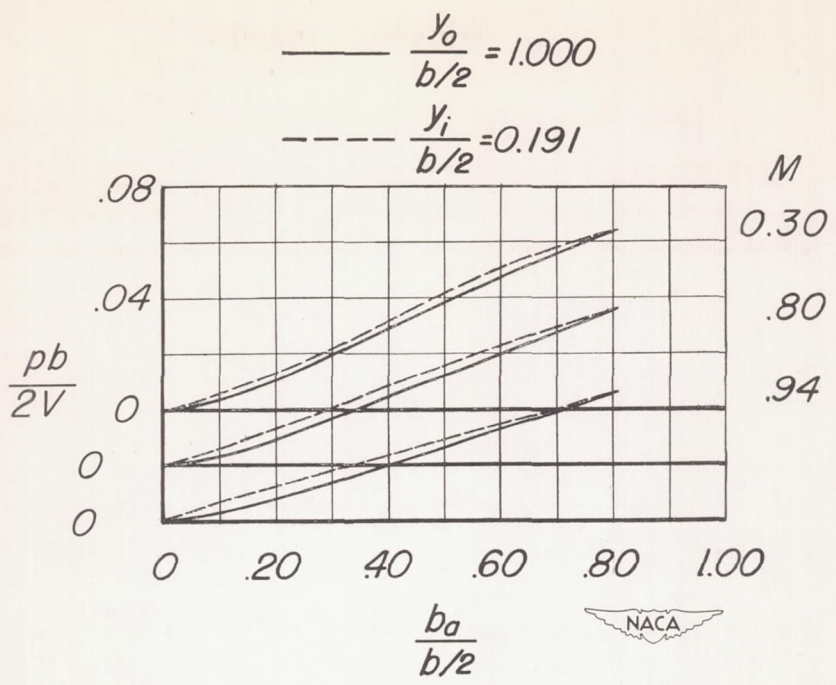


Figure 9.- Variation of the rolling effectiveness with aileron span and spanwise location. $\delta_a = 5.07°$.

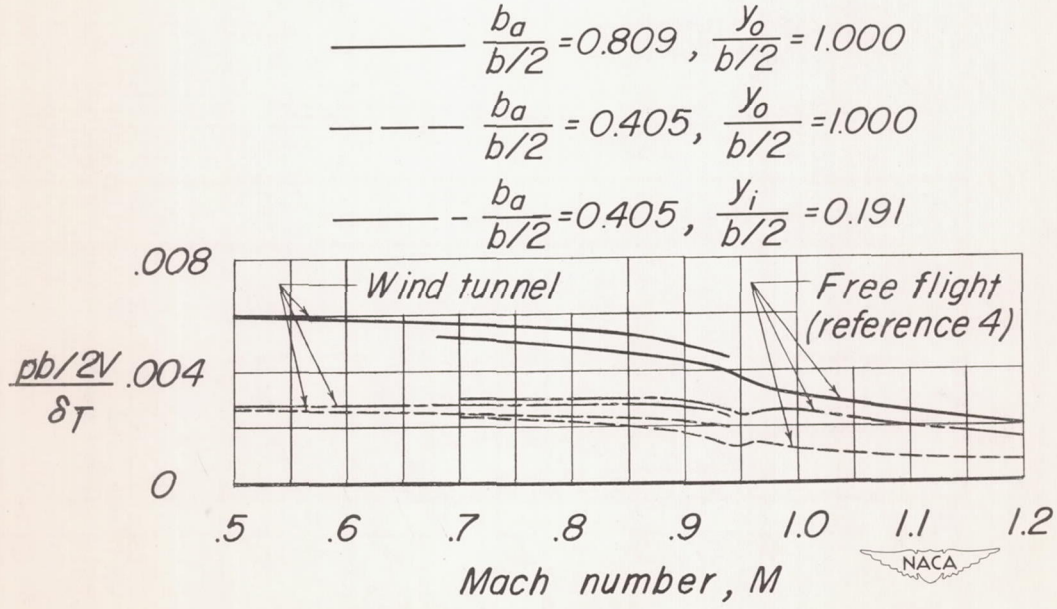


Figure 10.- Comparison of the rolling effectiveness as determined by wind-tunnel and free-flight testing techniques.

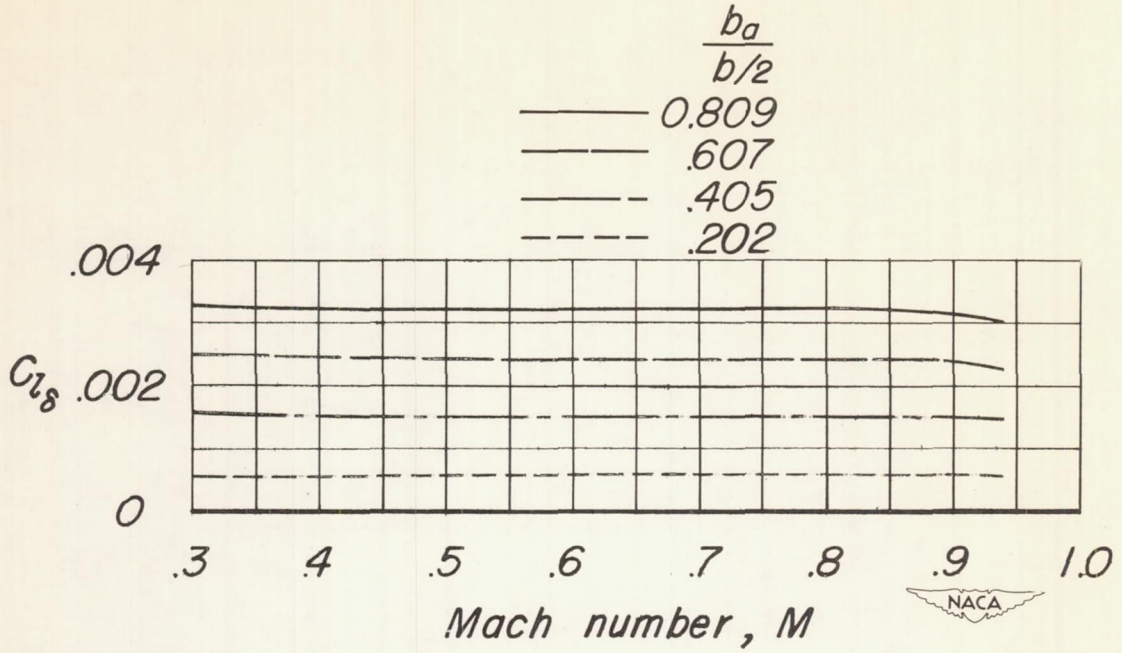


Figure 11.- Effect of aileron span on the variation of the aileron effectiveness parameter C_{l_δ} with Mach number. $y_o = 1.000\frac{b}{2}$.

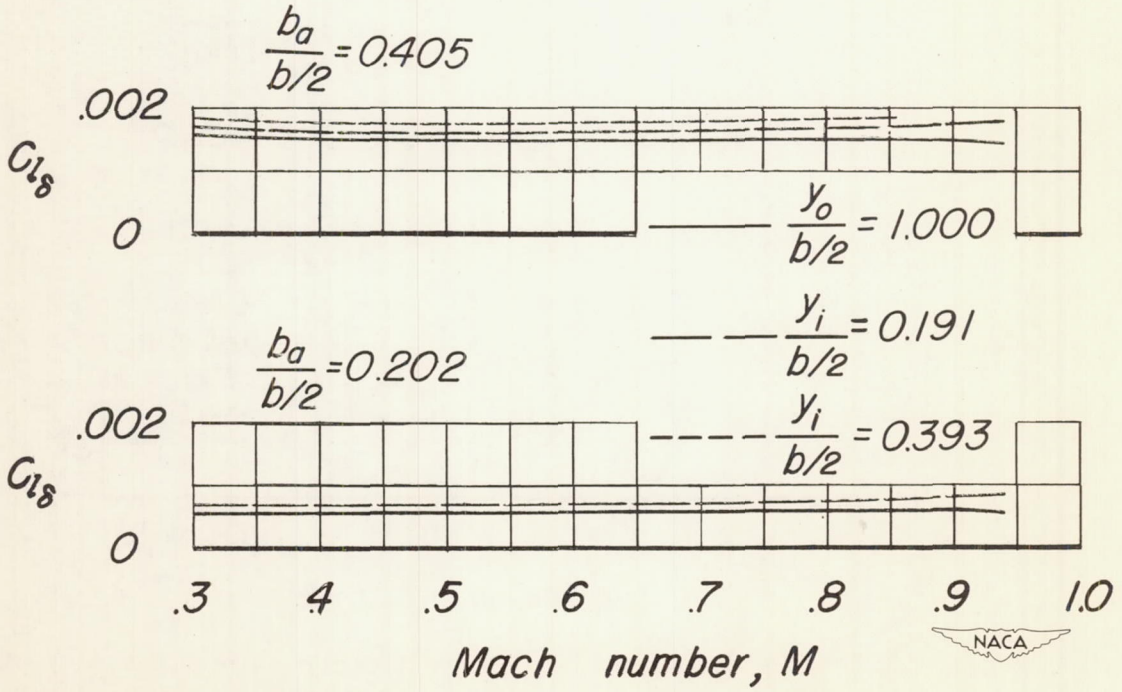


Figure 12.- Effect of spanwise aileron location on the variation of the aileron effectiveness parameter C_{l_δ} with Mach number.

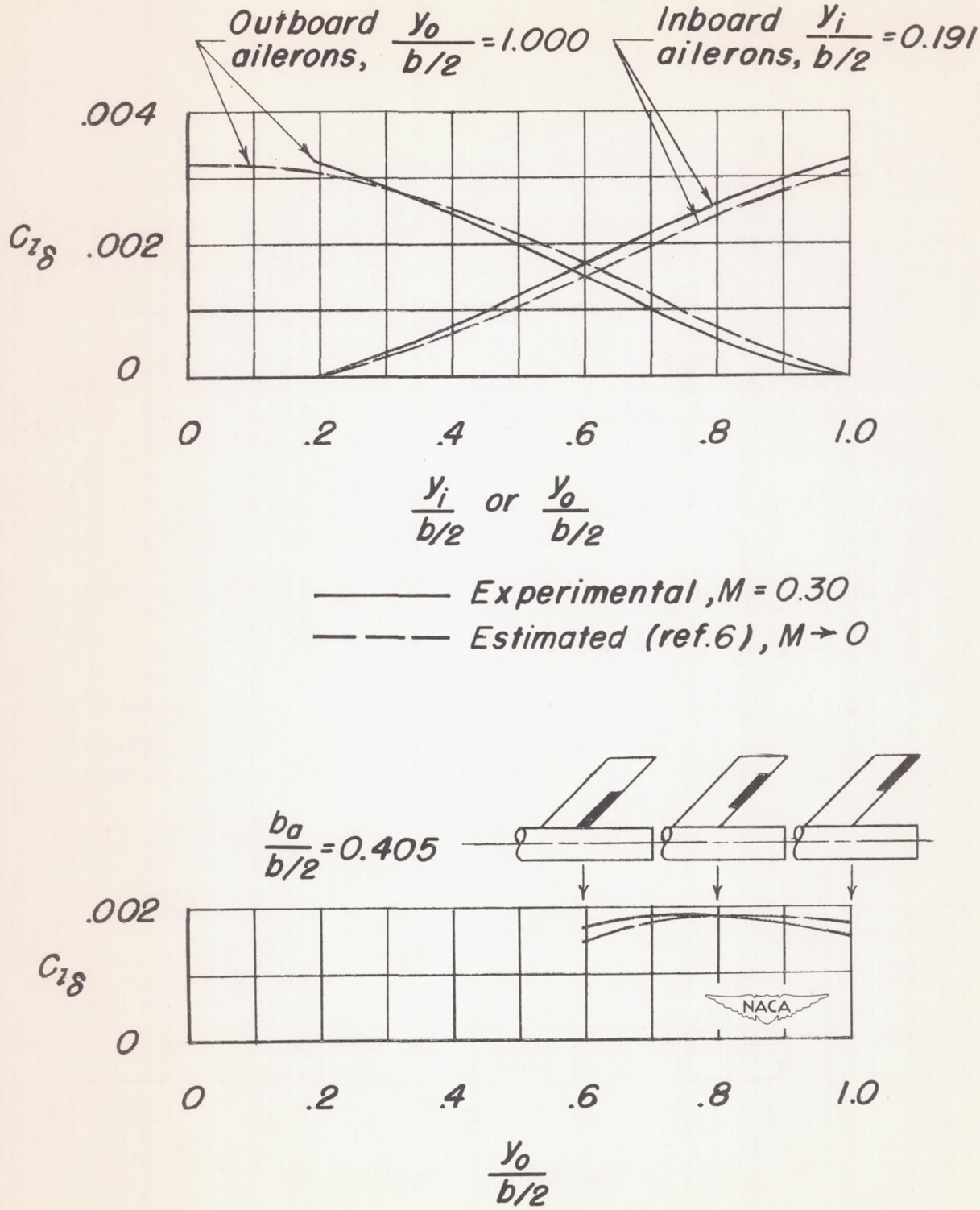


Figure 13.- Comparison of the experimental and estimated aileron effectiveness parameters.

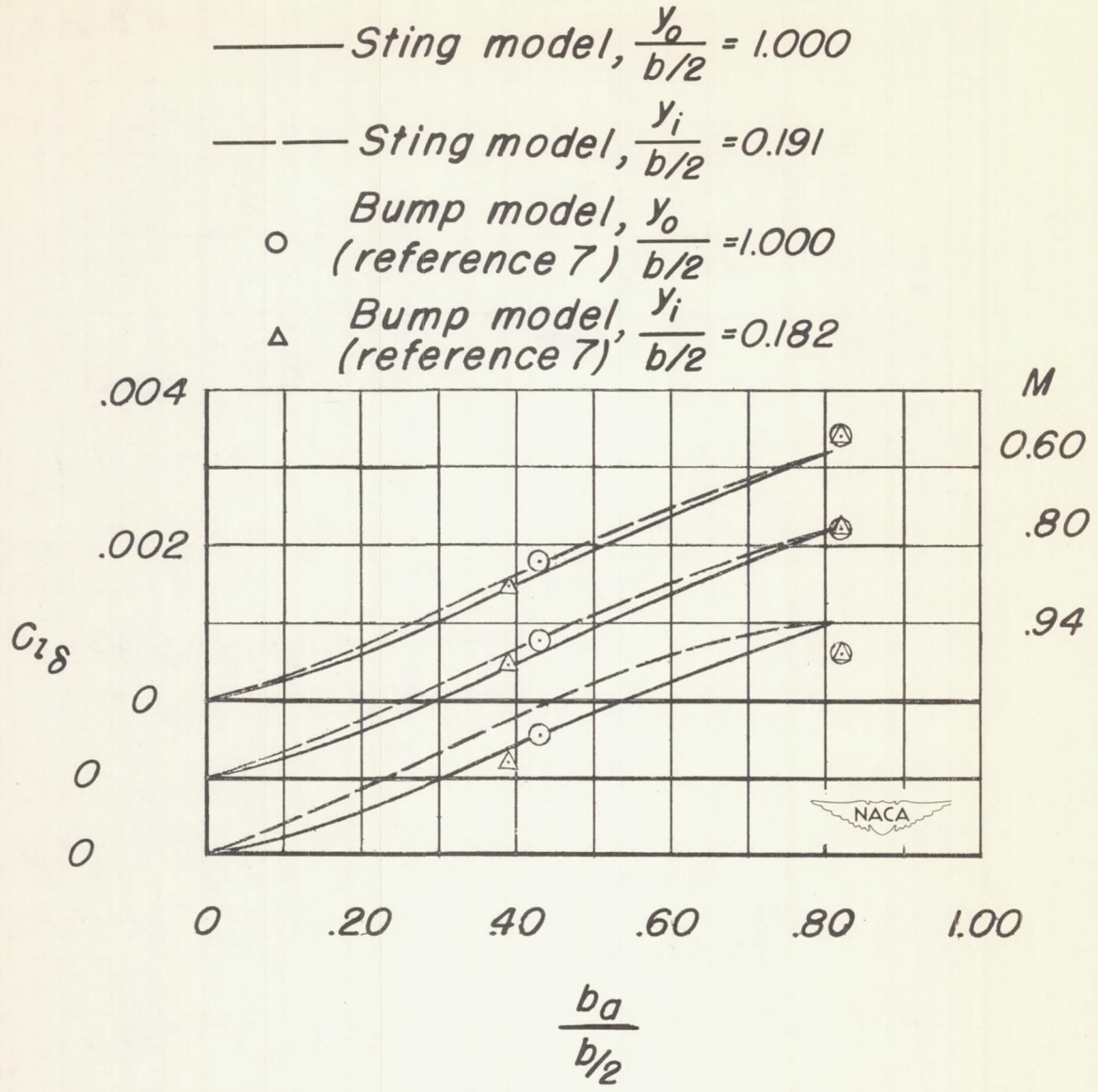


Figure 14.- Comparison of the aileron effectiveness parameters as determined by the sting and transonic-bump testing techniques.